厚生労働科学研究費補助金（新興再興研究事業）
平成19年度 分担報告書
アジアで流行している感染症の我が国への侵入監視の強化に関する研究

わが国およびアジアのクリプトスポリジウム汚染状況の分子疫学的調査

分担研究者　中井　裕　　東北大学大学院農学研究科

研究要旨

海外からのクリプトスポリジウムの侵入監視のためには、わが国の汚染状況を知る必要がある。そこで、わが国のウシおよび野生動物の汚染調査および分離原虫の遺伝子解析を実施した。アジアおよびエジプトにおけるクリプトスポリジウムの汚染状況を知るために、現地の研究者との共同研究により調査を行った。海外からの伝播経路の一つである渡り鳥としてのツルに注目して、クリプトスポリジウムの調査を実施した。さらにわが国に侵入した場合の、原虫の殺滅方法として、光触媒繊維モジュールのクリプトスポリジウムに対する効果を観察した。

1．北海道のと畜場に搬入されたウシ325頭、ブタ108頭の直腸便の検査を行い、成牛5頭からオーシストを検出した。18S rRNA遺伝子配列決定とSCIDマウスへの感染性から、*Cryptosporidium andersoni* Kawatabi typeと同定し、この型の原虫が本州および北海道に存在することを明らかにした(13)。

2．ウシ飼養場の草地で捕獲したアカネズミからオーシストを検出した。遺伝子配列、マウスおよびアカネズミに対する感染性ともに*C. muris*とはやや異なるものの、その差異は大きくないことから、新しい*C. muris*のgenotypeとして扱うこととし、large Japanese field mouse genotypeと命名した(12)。

3．*C. paruvum*オーシストの感染性の評価にはprepatent periodの観察が有効で、少ない頭数のSCIDマウスで感染性評価が可能であることを明らかにした(11)。

4．わが国の標準株である*C. paruvum* HNJ-1が*C. paruvum*（従来の呼称ではgenotype 2またはウシ型）であることと、既報の*C. paruvum*と異なる部分配列をもつことを明らかにした(10)。

5．ウシの胃に感染する*C. andersoni* Kawatabi typeの疫学研究を継続して実施し、感染牛の病理学的解析を行った(6)。

6．宮城県において、動物管理施設などに搬入された294頭のイヌおよびネコ31頭の糞便検査を実施し、1頭のイヌから*Cryptosporidium*オーシストの分離に成功した。18S rRNA遺伝子の全長解析による、わが国初の*C. canis*の同定例となった(5)。

7．わが国に飛来するナベヅル、マナヅル、北海道の留鳥であるタンチョウの糞便から*Eimeria*型のコクシジウムを検出し、遺伝子解析を行った(4)。
8．*Cryptosporidium*種の鑑別にDGGE法による遺伝子解析が有効であることを明らかにした(3)。
9．アジアにおける*Cryptosporidium*の汚染調査のため、中央ベトナム獣医学研究所および中国河南農業大学と共同研究を行った。とくに、ベトナムのウシに*C. paruvum*および*C. andersoni*が蔓延していることをオーシストの形態学的観察および遺伝子解析で明らかにした(2)。
10．光触媒繊維モジュールは*C. parvum*オーシストに対して高い殺滅効果を持つことを明らかにした（1)。
これらの研究を通して、国内外における、クリプトスポリジウムの汚染状況調査を高い精度で実施する研究体制が整えられた。しかし、アジアおよび諸外国のクリプトスポリジウム汚染実態の調査は緒についたに過ぎない。今後、諸外国におけるクリプトスポリジウムの流行状況を把握するためには、海外研究拠点と連携した調査の継続、調査範囲の拡大が必須である。また、渡り鳥などに対するモニタリングの継続および強化も必要と考えられた。

A. 研究目的

アジアからの*Cryptosporidium*の侵入を監視するためには、国内における本原虫分布の現状を明確にしておく必要がある。まず、国内における*Cryptosporidium*の浸潤状況を把握するため、調査を実施する。アジアおよびアフリカに関しては、中国、ベトナム、エジプトを対象として調査を行う。渡り鳥としてのツルに注目して*Cryptosporidium*の感染状況を調査する。また、*Cryptosporidium*の蔓延を防止するためにはオーシストの殺滅が重要であるため、細菌に対して高い殺滅作用を示す光触媒繊維モジュールの有効性を観察する。

B. 研究方法

と畜場および動物愛護センターに搬入されたウシ、イヌおよびネコについて、ショ糖浮遊法により糞便検査を行った。陽性サンプルに関しては、DNAを抽出し、PCR法によって18S rRNA遺伝子を増幅し、塩基配列を決定した。SCIDマウスを用いて、感染性を観察した。ベトナムにおいては、農家に飼養されるウシの、月齢、下痢の有無を記載して糞便サンプルを採取し、Ziehl Neelsen変法によってオーシストを検出した。*C. parvum*型オーシストが検出された1検体については、上記の方法で18S rRNA遺伝子の塩基配列を決定した。エジプトにおいては、ウシふん便を対象に、現地で浮遊法を実施し、クリプトスポリジウムの種の簡易同定を行い、遺伝子解析で確定することとした。ナベヅル、マナヅルに関しては、鹿児島県出水市の飛来地、タンチョウに関しては、釧路市において糞便を採取し、浮遊法により原虫を観察し、分離したオーシストに関して遺伝子解析を行った。光触媒繊

維を装備したアクアソリューション®（宇部興産（株）製 UPM-25408-80P）に *C. parvum* HNJ-1 株オーシストの浮遊液を通過させ、暴露されたオーシストを SCID マウスに経口感染させて、オーシストの感染性を観察した。

C. 研究結果

１．北海道のと畜場に搬入されたウシ 325 頭、ブタ 108 頭の直腸便の検査を行い、成牛 5 頭からオーシストを検出した。18S rRNA 遺伝子配列決定と SCID マウスへの感染性から、*Cryptosporidium andersoni* Kawatabi type と同定し、この型の原虫が本州および北海道に存在することを明らかにした。

２．ウシ飼養場の草地で捕獲したアカネズミからオーシストを検出した。遺伝子配列、マウスおよびアカネズミに対する感染性ともに *C. muris* とはやや異なるものの、その差異は大きくないことから、新しい *C. muris* の genotype として扱うこととし、large Japanese field mouse genotype と命名した。

３．*C. parvum* オーシストの感染性の評価には prepatent period の観察が有効で、少ない頭数の SCID マウスで感染性評価が可能であることを明らかにした。

４．わが国の標準株である *C. parvum* HNJ-1 が *C. parvum*（従来の呼称では genotype 2 またはウシ型）であることと、既報の *C. parvum* と異なる部分配列をもつことを明らかにした。

５．ウシの胃に感染する *C. andersoni* Kawatabi type の疫学研究を継続して実施し、感染牛の病理学的解析を行った。

６．宮城県において、動物管理施設などに搬入された 294 頭のイヌおよびネコ 31 頭の糞便検査を実施し、1 頭のイヌから *Cryptosporidium* オーシストの分離に成功した。18S rRNA 遺伝子の全長解析による、わが国初の *C. canis* の同定例となった。

７．わが国に飛来するナベヅル、マナヅル、北海道の留鳥であるタンチョウの糞便から *Eimeria* 型のコクシジウムを検出し、遺伝子解析を行った。

８．*Cryptosporidium* 種の鑑別に DGGE 法による遺伝子解析が有効であることを明らかにした(3)。

９．アジアにおける *Cryptosporidium* の汚染調査のため、中央ベトナム獣医学研究所および中国河南農業大学と共同研究を行った。とくに、ベトナムのウシに *C. parvum* および *C. andersoni* が蔓延していることをオーシストの形態学的観察および遺伝子解析で明らかにした。

10.　光触媒繊維モジュールは *C. parvum* オーシストに対して高い殺滅効果を持つことを明らかにした。

D. 考察

わが国のイヌの *Cryptosporidium* の分子疫学的調査：

Cryptosporidium 陽性のイヌは、ウシ飼養地域で捕獲されたものであったが、検出されたオーシストは *C. canis* であり、感染にウシは関与していないと考えられた。18S rRNA 遺伝子配列は、米国分離株の配列と 2 塩基置換が認められ、異なる

株であることが明らかとなった。Abe ら（J.Bet.Med.Sci, 64:165-168, 2002）は大阪においてイヌから *C. canis* の分離を報告している。彼らは 18S rRNA 遺伝子配列の 289bp を決定したが、本研究では全長の 1741bp を決定しており、*C. canis* がわが国に存在することを明確に示すものであり、東北地方からの検出は初である。また、米国株と一部の配列が異なることを明らかにし、*C. canis* には遺伝的に異なる株が存在し、多様性があることが明らかとなった。なお、わが国の *C. canis* に関して、ヒトへの感染性は明確ではなく、今後の検討が必要である。

アジアにおける *Cryptosporidium* の調査：

ベトナムのウシにおいてもわが国同様に *C. parvum*（bovine genotype）が存在することから、ヒトへの感染の危険があることが明らかとなった。分離株に関しては、18S rRNA 遺伝子の DNA 配列がわが国で分離されている株と同一であった。したがって、この株がわが国に侵入した場合、本遺伝子以外の遺伝子の解析によって鑑別する必要がある。

エジプトのサンプルは現在解析中であり、詳細は、まとめて来年度発表する予定である。

ツルの原虫感染状況調査：

ツルは *Cryptosporidium* を媒介しない可能性が高いと考えられたが、感染症の我が国への侵入監視の観点からは、ロシア、中国、朝鮮半島を経て日本に移動するナベヅルおよびマナヅルに関するモニタリングは今後も必要と考えられる。

光触媒繊維モジュールの *Cryptosporidium* 殺滅効果：

光触媒繊維モジュールは *C. parvum* HNJ-1 株オーシストに対して高い殺滅効果を持つことが分かった。ここで光触媒繊維と紫外線の相乗効果が発揮されたか否かは不明であるが、光触媒繊維モジュールは汚水の濁度改善効果を有することが知られており、紫外線のみでは困難とされる汚水に含まれるオーシストの殺滅への応用が期待される。

E.結論

わが国には米国分離株と同じ 18S rRNA 遺伝子を有するが、マウス感染性が異なる *C. andersoni* が存在する。

わが国固有の野生ネズミであるアカネズミは、従来のラット由来の *C. muris* と異なる性質を持つ *C. muris* large Japanese field mouse genotype を持つ。

わが国の標準株である *C.parvum* HNJ-1 は *C.parvum*（従来の呼称では genotype 2 またはウシ型）であり、既報の *C.parvum* の 18S rRNA 遺伝子と異なる部分配列を有する。

わが国には米国分離株と異なる 18S rRNA 遺伝子を有するイヌ由来の *C. canis* が存在する。

ベトナムにはわが国の分離株に類似した *C. parvum*（bovine genotype）が存在する。

ベトナムにはわが国同様にウシ固有種と考えられている *C. andersoni* 型が存在する。

ナベヅル、マナヅル、タンチョウは *Cryptosporidium* を媒介しない可能性が高いが、ツル固有の *Eimeria* 原虫を有する。
光触媒繊維モジュールは *C. parvum* オーシストに対して高い殺滅効果を持つ。

F.健康危機情報

クリプトスポリジウムに関しては、健康危機的状況とは言えないと考える。

しかし、今回ウシから検出された *C. andersoni* は英国において健康なヒトから検出された例があり、ヒトへの感染性を含めて詳しい解析を行う必要がある。また、アジアにおけるクリプトスポリジウムの流行状況を把握するためには、海外研究拠点との連携を深め、調査の継続、調査範囲の拡大が必須である。また、渡り鳥などに対するモニタリングの継続および強化も必要と考えられる。

G.研究発表

1．論文発表

1) Endo M, Honma H, Ozutsumi Y, Otawa K, Yamaoka H, Nakai Y. Inactivation of *Cryptosporidium parvum* by using the photocatalytic reactor. Water Research, submitted (2008)
2) Nguyen ST, Nguyen DT, Le DQ, Hua LNL, Nguyen TV, Honma H, Nakai Y. Prevalence and first genetic identification of *Cryptosporidium* spp. in cattle in central Viet Nam. Vet. Parasitol., in press 150 (4), 357-361 (2007)
3) Satoh M, Nakai Y. Discrimination of *Cryptosporidium* species by denaturing gradient gel electrophoresis. Parasitol. Res., 101(2), 463-466 (2007)
4) Honma H, Yokoyama T, Inoue M, Uebayashi A, Matsumoto F, Watanabe Y, Nakai Y. Genetical identification of coccidia in red-crowned crane, *Grus japonensis*. Parasitol. Res., 100(3),637-640 (2007)
5) Satoh M, Matsubara-Nihei Y, Sasaki T, Nakai Y. Characterization of *Cryptosporidium canis* isolated in Japan. Parasitol. Res., 99(6), 746-748 (2006)
6) Masuno K., Yanai T, Hirata A, Yonemaru K, Sakai M, Satoh M, Masegi T, Nakai Y. Morphological and immunohistochemical features of *Cryptosporidium andersoni* in cattle. Vet. Pathol.. 43, 202-207 (2006)
7) Nakai Y, Satoh M, Koyama Y, Hikosaka K, Takahashi J, Suzuki C, Masuno K, Yanai T. Genetical and biological charactristics of gastric *Cryptosporidium* spp. ICOPA XI Programme, 75, Glasgow, Scotland, UK, August (2006)
8) Honma H, Yokoyama T, Nakai Y. Morphological and genetical identification of coccidia in cranes in Japan. ICOPA XI Programme, 70, Glasgow, Scotland,

UK, 6-11 August (2006)

9) Suzuki C, Takahashi J, Sasaki T. Yamaoka H, Nakai Y. Disinfection of *Cryptosporidium* oocysts by photocatalytic fiber. 3rd International Workshop on Water-borne Protozoan Parasites, ICOPA XI Programme, 80, Glasgow, Scotland, August (2006)

10) Satoh M, Kimata I, Iseki M, Nakai Y. Gene analysis of *Cryptosporidium parvum* HNJ-1 strain isolated in Japan. Parasitol. Res., 97 (6), 452-457 (2005)

11) Hikosaka K, Satoh M, Koyama Y, Nakai Y. Quantification of the infectivity of *Cryptosporidium parvum* by monitoring the oocyst discharge from SCID mice. Vet. Parasitol., 134, 173-176 (2005)

12) Hikosaka K, Nakai Y. A novel genotype of *Cryptosporidium muris* from large Japanese field mice, Apodemus speciosus. Parasitol. Res., 97 (5), 373-379 (2005)

13) Koyama Y, Satoh M, Maekawa K, Hikosaka K, Nakai Y. Isolation of *Cryptosporidium andersoni* Kawatabi type in a slaughterhouse in the northern island of Japan. Vet. Parasitol., 130: 323-326 (2005)

研究成果の刊行に関する一覧表(平成１７－１９年度)　　プロジェクト３：原虫

執筆者氏名	刊行書籍又は雑誌名 (雑誌のときは雑誌名、 巻号数、論文名)	刊行書店名	巻名	ページ	刊行年
マラリア					
Jongwutiwes S, Putaporntip C, Iwasaki T, Ferreira MU, Kanbara H, Hughes AL.	Mitochondrial Genome Sequences Support Ancient Population Expansion in *Plasmodium vivax*	*Mol. Biol. Evol.*	22	1733-1739	2005
Yoes P, Dachlan YP, Yotopranoto S, Sutanto BV, Santoso Sri HB, Widodo AS, Sutanto A, Gerudung IKK, Takagi M, Tsuda Y, Tanabe K, Kawamoto F, Yoshinaga K, Kanbara H.	Malaria endemic patterns on Lombok and Sumbawa islands, Indonesia.	*Trop. Med. & Hlth*	33	105-113	2005
Matsuoka H, Nguon C, Kanbe T, Jalloh A, Sato H, Yoshida S, Hirai M, Arai M, Socheat D, Kawamoto F.	Glucose-6-phosphate dehydrogenase (G6PD) mutations in Cambodia: G6PD Viangchan (871G>A) is the most common variant in the Cambodian population.	*J. Human Genet.*	50	468-472	2005
Arakawa T, Komesu A, Otsuki A, Sattabongkot J, Udomsangpetch R, Matsumoto Y, Tsuji N, Wu Y, Torii M, Tsuboi T.	Nasal immunization with a malaria transmission-blocking vaccine candidate, Pfs25, induces complete protective immunity in mice against field isolates of *Plasmodium falciparum*.	*Infect. Immun.*	73	7375-7380	2005
ngruang T,	Erythrocyte surface	*Mol. Biochem.*	140	13-21	2005

Kaneko O, Murakami Y, Tsuboi T, Hamamoto H, Akimitsu N, Sekimizu K, Kinoshita T, Torii M.	glycosylphosphatidyl inositol anchored receptor for the malaria parasite.	*Parasitol.*			
Kaneko O, Yim-Lim BYS, Iriko H, Ling IT, Otsuki H, Grainger M, Tsuboi T, Adams JH, Mattei D, Holder AA, Torii	Apical expression of three RhopH1/Clag proteins as components of the *Plasmodium falciparum* RhopH complex.	*Mol. Biochem. Parasitol*	143	20-28	2005
Asahi H, Kanazawa T, Hirayama N, Kajihara Y.	Investigating serum factors promoting erythrocytic growth of *Plasmodium falciparum.*	*Experimental Parasitology*	109	7-15	2005
Sakihama N, Ohmae H, Bakote'e B, Kawabata M, Hirayama K. Tanabe K.	Limited allelic diversity of *Plasmodium falciparum msp1* from populations in the Solomon Islands, a highly endemic area.	*Am. J. Trop. Med. Hyg.*	74	31-40	2006
Fyjita K, Chen TT, Nishina T, Ishikawa H.	Fyjita K, Chen TT, Nishina T, Ishikawa H. Modeling of Re-emerging Plasmodium vivax in the Northern Area of the Republic of Korea based on a mathematical model.	*J. Fac.* Environmental Sci. & Tech. Okayama U.	11	1-7	2006
Jalloh A, Thien HV, Ferreira MU, Ohashi J, Matsuoka H, Kanbe T, Kikuchi A,	Sequence variation in the T-cell epitopes of the *Plasmodium falciparum* circumsporzoite protein (CSP) among field isolates is temporally stable: a five-year longitudinal study in	*J. Clin. Microbiol*	44	1229-1235	2006

Kawamoto F.	Southern Vietnam.				
Putaporntip C, Jongwutiwes S, Iwasaki T, Kanbara H, Hughes AL.	Short communication: Ancient common ancestry of the merozoite surface protein 1 of *Plasmodium vivax* as inferred from its homologue in *Plasmodium knowlesi*.	*Mol. Bio. Parasitol.*	148	32-33	2006
Yano K, Komaki-Yasuda K, Tsuboi T, Torii M, Kano S, Kawazu S.	2-Cys Peroxiredoxin TPx-1 is involved in gametocyte development in *Plasmodium berghei*.	*Mol. Biochem. Parasitol.*	148	44-51	2006
Kaneko O, Templeton TJ, Iriko H, Tachibana M, Otsuki H, Takeo S, Sattabongkot J, Torii M, Tsuboi T.	The *Plasmodium vivax* homolog of the ookinete adhesive micronemal protein, CTRP.	*Parasitol. Int.*	55	227-231	2006
Palacpac NM, Leung BW, Arisue N, Tanabe K, Sattabongkot J, Tsuboi T, Torii M, Udomsangpetch R, Horii T.	*Plasmodium vivax* serine repeat antigen (SERA) multigene family exhibits similar expression patterns in independent infections.	*Mol. Biochem. Parasitol.*	150	353-358	2006
Han ET, Lee DH, Park KD, Seok WS, Kim YS, Tsuboi T, Shin EH, Chai JY.	Reemerging vivax malaria: changing patterns of annual incidence and control programs in the Republic of Korea.	*Korean J. Parasitol.*	44	285-294	2006
Fujita K, Chen TT, Nishina T and Ishikawa H.	Modeling of Re-emerging *Plasmodium vivax* in the Northern Area of the Republic of Korea Based on a Mathematical Model	*J. Fac. Environmental Sci. & Tech. Okayama U.*	11(1)	1-7	2006
Arai M., Kawamoto F., *et al.*	Reactivity of blood samples spotted onto filter papers in the WST-8 method for screening of G6PD deficiency.	*Acta Medica Okayama,*	60	127-134	2006

Jalloh, A., Kawamoto, F., et al.	equence variation in the T-cell epitopes of the *Plasmodium falciparum* circum- sporozoite (CS) protein among field isolates is temporally stable: a five-year longitudinal study in Southern Vietnam.	*J. Clin. Microbiol.*	44	1229-1235	2006
Kawamoto, F., et al.	Further investigations of glucose-6-phosphate dehydrogenase variants in Flores Island, eastern Indonesia.	*J. Human Genet*	51	952-957	2006
Mita T, Kaneko A, Hwaihawanje I, Tsukahara T, Takahashi N, Osawa H, Tanabe K, Kobayakawa T, Björkman A.	A. Rapid selection of dhfr mutant allele in *P. falciparum* isolates after the introduction of sulfadoxine/pyrimethamine in combination with 4-aminoquinolines in Papuea New Guninea.	*Inf. Gen. Evol.*	6	447-452	2006
Mita T, Tanabe K, Takahashi N, Tsukahara T, Eto H, Dysoley L, Ohmae H, Kita K, Krudsood S, Looareesuwan S Kaneko A, Bjorkman A, Kobayakawa T.	Independent evolution of Pyrimethamine resistance on *Plamodium falciparum* isolates in Melanesia	*Antimicrob Agents Chemother.*	Mar; 51(3)	1071-1077	2007
Tanabe K, Escalante A, Sakihama N, Honda M, Arisue N, Horii T, Culleton R, Hayakawa T, Hashimoto T, Longacre S, Pathirana S, Handunnetti S,	ecent independent evolution of *msp1* polymorphism in *Plamsodium vivax* and related malaria parasirtes.	*Mol. Biochem. Parasitol.*	156	74-79	2007

Kishino H.					
Arizono N, Nakanishi K, Horii T, Tanabe K.	Progress in the molecular biology and the immunology of nematode infections.	*Trends Parasitol*	23	175-181.	2007
Sakihama N, Nakamura M, Palanca AA Jr, Argubano RA, Realon EP, Larracas AL, Espina RL, Tanabe K.	Allelic diversity in the merozoite surface protein 1 gene of *Plasmodium falciparum* on Palawan Island, the Philippines.	*Parasitol. Int*	56	185-194	2007
Tanabe K, Sakihama N, Walliker D, Babiker H, Abdel-Muhsin AA, Bakote'e B, Ohmae H, Arisue N, Horii T, Rooth I, Färnert A, Björkman A, Ranford-Cartwright L.	Allelic dimorphism-associated restriction of recombination in *Plasmodium falciparum msp1.*	*Gene*	392	153-160	2007
Tanabe K, Sakihama N, Rooth I, Björkman A, Färnert A.	High frequency of recombination-drived allelic diversity and temporal variation of *Plasmodium falciparum* in Tanzania.	*Am. J. Trop. Med. Hyg.*	76	1037-1045	2007
Cheng Y, Hayasaka H, Watanabe K, Tao Y, Liu J, Tsukamoto H, Horii T, Tanabe K, Tachibana H	Production of High-Affinity Human Monoclonal Antibody Fab Fragments to the 19-Kilodalton C-Terminal Merozoite Surface Protein 1 of *Plasmodium falciparum.*	*Infect. Immun.*	75	3614-3620	2007
Pacheco MA, Poe AC, Collins WE, A. Lal AA,	Comparative study of the genetic diversity of the 42 kDa fragment of the merozoite surface protein 1	*Inf. Gen. Evol.*	7	180-187	2007

Tanabe K, Udhayakumar V, Escalante A.	in *Plasmodium falciparum* and *P. vivax*.				
T, Tanabe K, Takahashi N, Dysoley L, Eto F, Hwaihwanje I, Ohmae H, Kita K, Looareesuwan S, Kaneko A, Björkman A, Kobayakawa T.	Independent unique evolution of pyrimethamine resistance of *P. falciparum* in Melanesia.Mita	*Antimicrob. Agents Chemother.*	51	1071-1077	2007
Mudeppa DG, Pang CKT, Tsuboi T, Endo Y, Buckner FS, Varani G, Rathod PK.	Cell-free production of functional *Plasmodium falciparum* dihydrofolate reductase-thymidylate synthase.	*Mol. Biochem. Parasitol.*	151	216-219.	2007
Ghoneim A, Kaneko O, Tsuboi T, Torii M.	The *Plasmodium falciparum* RhopH2 promoter and first 24 amino acids are sufficient to target proteins to the rhoptries.	*Parasitol. Int.*	56	31-43	2007
Kobayashi F, Waki S, Niikura M, Tachibana Mayumi, Tsuboi T, Torii M, Kamiya S.	*Plasmodium berghei* XAT: Protective 155/160 kDa antigens are located in Parasitophorous vacuoles of schizont-stage parasite.	*Exp. Parasitol.*	116	450-457.	2007
Han ET, Watanabe R, Sattabongkot J, Khuntirat B, Sirichaisinthop J, Iriko H, Jin L, Takeo S, Tsuboi T.	Detection of four *Plasmodium* species by genus- and species-specific loop-mediated isothermal amplification for clinical diagnosis.	*J Clin Microbiol.*	45	2521-2528	2007
Chen TT, Nishina T, Hisakane N, Ohmae H, Ishikawa H.	A mathematical model of *Plasmodium falciparum* transmission making allowance for drug resistance: Simulations in the situation of The Solomon	*Tropical Medicine and Health*,	35(2)	217	2007

	Islands.				
Matsuoka H, Thuan DTV, Thien HV, Kanbe T, Jalloh A, Hirai M, Arai M, Dung NT, Kawamoto F.	Seven different glucose-6-phosphate dehydrogenase variants including a new variant distributed in Lam Dong Provinve in Southern Vietnam.	*Acta Medica Okayama,*	61	213-219	2007
Ikuta K, Torimoto E, Inamura H, Shindo M, Sato T, Kawamoto F, Yamasaki H, Kohgo H:	A case of imported tertian malaria occurred despite prophylaxis by mefloquine in East Timor.	*J. BTHA,*	10	50-51	2007
Karunaweera ND, Ferreira MU, Munasinghe A, Barnwell JW, Collins WE, King CL, Kawamoto F, Hartl DL, Wirth DF	Extensive microsatellite diversity in the human malaria parasite *Plasmodium vivax.*	*Gene*	410	105-112	2007
Iriko H, Kaneko H, Otsuki H, Tsuboi T, X-z. Su, Tanabe K, Torii M.	Diversity and evolution of the highly diverse rhoph1/clag multigene family of *Plasmodium falciparum.*	*Mol. Biochem. Parasitol.*	158	11-21	2008
木村幹男	特集 話題の感染症. 6. 海外旅行と輸入感染症	INFECTION CONTROL	14	531-535	2005
重松美加, 菊池 均, 木村幹男	特集 海外旅行と感染症. I. 渡航者感染症およびその取り組みの現状	化学療法の領域	21	1401-1407	2005
大前比呂思, 遠藤卓郎, 長谷山路夫, 新妻淳, 飯塚信二, 津田良夫	検疫感染症としてのマラリアをどう捉えるか	*Clinical Parasitol*	17	127-130	2006
木村幹男, 波川京子	日本の旅行者におけるマラリア予防.	病原微生物検出情報	21	4-6	2007

陳甜甜、仁科朝彦、久兼直人、石川洋文	クロロキン薬剤耐性に関する熱帯熱マラリア数理モデル解析．－ソロモン諸島を対象としたシミュレーション	*J. Fac. Environmental Sci. & Tech. Okayama U.*	12(1)	19-27	2007
三浦彰子，新妻淳，大前比呂思.	マラリア感染蚊からの効率的な遺伝子検出の検討.	*日本検疫医学会誌*	9	118-122	2007
大前比呂思，亀井喜世子，中澤港 Bernard Bakote'e	マラリア対策の進捗による感染状況の変化とフィールドでの迅速診断キットの限界	*Clinical Parasitol*	18	76-79	2008
原虫					
Natividad FF, Buerano CC, Lago CB, Mapua CA, de Guzman BB, Izumiyama S, Yagita K, Seraspe EB, Samentar LP, Matias RR, and Endo T.	Prevalence of *Giardia* and *Cryptosporidium* in Stool Samples of Diarrheic Patients from the Philippines		in preparation		2008
Jongwutiwes S, Putaporntip C, Charoenkor M, Izumiyama S, and Endo T.	Molecular epidemiology of cryptosporidiosis in Thailand: Analysis of the SSU rRNA and Cpg60/45/15 sequences		in preparation		2008
Endo M, Honma H, Ozutsumi Y, Otawa K, Yamaoka H, Nakai Y.	Inactivation of *Cryptosporidium parvum* by using the photocatalytic reactor.	Water Research,	submitted		2008
Honma H, Yokoyama T, Inoue M, Uebayashi A, Matsumoto F, Watanabe Y, Nakai Y.	Genetical identification of coccidia in red-crowned crane, *Grus japonensis*.	Parasitol. Res.	100(3),	637-640	2007

Nguyen ST, Nguyen DT, Le DQ, Hua LNL, Nguyen TV, Honma H, Nakai Y.	Prevalence and first genetic identification of *Cryptosporidium* spp. in cattle in central Viet Nam.	Vet. Parasitol.,	150 (4)	357-466	2007
Satoh M, Nakai Y.	Discrimination of *Cryptosporidium* species by denaturing gradient gel electrophoresis.	Parasitol. Res.	101(2),	463-466	2007
T. Izumi, K. Yagita, T. Endo, T. Ohyama.	Detection System of *Cryptosporidium parvum* Oocysts by Brackish Water Benthic Shellfish (*Corbicula japonica*) as a Biological Indicator in River Water.	Arch. Environ. Contam. Toxicol.,	51	559-566	2006
Tadashi Itagaki, Shisuka Kinoshita, Mikiko Aoki, Naoyuki Itoh, Hideharu Saeki, Naoto Sato, Junya Uetsuki, Shinji Izumiyama, Kenji Yagita, Takuro Endo.	Genotyping of *Giardia intestinalis* from domestic and wild animals in Japan using glutamete dehydrogenase gene sequencing.	Veterinary Parasitology.	133	283-287	2005
高木正明、鳥海 宏、遠藤卓郎、山本徳栄、黒木俊郎	プールを介したクリプトスポリジウム症集団発生事例	感染症学雑誌	82	14-19	2008
遠藤卓郎、泉山信司、八木田健司	□ 寄生虫・ウィルスを原因とする腸管感染症 4. 水泳プールを介したクリプトスポリジウム症感染.	化学療法の領域	23	148-152	2007

Available online at www.sciencedirect.com
SCIENCE DIRECT
ELSEVIER
Molecular & Biochemical Parasitology 140 (2005) 13–21
MOLECULAR & BIOCHEMICAL PARASITOLOGY

Erythrocyte surface glycosylphosphatidyl inositol anchored receptor for the malaria parasite

Thanaporn Rungruang[a], Osamu Kaneko[a,*], Yoshiko Murakami[b], Takafumi Tsuboi[a,c], Hiroshi Hamamoto[d], Nobuyoshi Akimitsu[d], Kazuhisa Sekimizu[d], Taroh Kinoshita[b], Motomi Torii[a]

[a] *Department of Molecular Parasitology, Ehime University School of Medicine, Toon, Ehime 791-0295, Japan*
[b] *Department of Immunoregulation, Research Institute for Microbial Diseases, Osaka University, Suita, Osaka 565-0871, Japan*
[c] *Cell-Free Science and Technology Research Center, Ehime University, Matsuyama, Ehime 790-8577, Japan*
[d] *Laboratory of Developmental Biochemistry, Graduate School of Pharmaceutical Sciences, The University of Tokyo, Tokyo 113-0033, Japan*

Received 29 August 2004; received in revised form 3 November 2004; accepted 4 November 2004
Available online 23 December 2004

Abstract

Parasitophorous vacuole formation is a critical step for the successful invasion of host erythrocytes by the malaria parasite. Rhoptry proteins are believed to have essential roles in vacuole formation, although their biological roles are poorly understood. To understand the molecular interactions between parasite rhoptry proteins and the erythrocyte during invasion, we have characterized the binding specificity of the high molecular mass rhoptry protein (RhopH) complex to erythrocytes using the rodent malaria parasite, *Plasmodium yoelii*. RhopH complex binding to erythrocytes was species-specific, observed with mouse but not rabbit or human erythrocytes. Binding is abolished following treatment of erythrocytes with trypsin or chymotrypsin. Because host cell cholesterol-rich membrane domains are recruited into the nascent parasitophorous vacuole, we evaluated a possible role of RhopH complex binding to the cholesterol-rich membrane domain-associated glycosylphosphatidyl inositol (GPI)-anchored protein. Using chimeric mice harboring GPI-deficient erythrocytes, RhopH complex binding to GPI-deficient mouse erythrocytes was undetectable, indicating involvement of GPI-anchored protein in *Py*RhopH complex binding. Furthermore, a significant reduction of *P. yoelii* parasite infection of GPI-deficient erythrocytes was observed in vivo, probably due to inefficient invasion. We conclude that the major erythrocyte receptor for *Py*RhopH complex is a protein attached to the erythrocyte surface via GPI-anchor and that GPI-deficient erythrocytes are resistant to *P. yoelii* invasion.

Keywords: Erythrocyte; GPI anchor; Invasion; Malaria; *Plasmodium yoelii*

1. Introduction

Malaria is one of the most prevalent and deadly global infectious diseases and is caused by the obligate intraerythrocytic stages of the protozoan parasite, *Plasmodium*. To facilitate erythrocyte invasion, *Plasmodium* merozoites discharge the contents of apical organelles called rhoptries that are involved in the formation of an intraerythrocytic parasitophorous vacuole in which the parasites reside and develop. The parasitophorous vacuole membrane (PVM) contains erythrocyte proteins found in detergent-resistant membrane [e.g., Duffy antigen receptor for chemokines (DARC) and glycosylphosphatidylinositol (GPI)-anchored proteins], but excludes most transmembrane proteins (e.g., glycophorin A) [1].

Abbreviations: DARC, Duffy antigen receptor for chemokines; EDTA, ethylenediaminetetraacetic acid; GPA, glycophorin A; mAb, monoclonal antibody; PBS, phosphate buffered saline

* Corresponding author. Tel.: +81 89 960 5286; fax: +81 89 960 5287.
E-mail address: okaneko@m.ehime-u.ac.jp (O. Kaneko).

0166-6851/$ – see front matter © 2004 Elsevier B.V. All rights reserved.
doi:10.1016/j.molbiopara.2004.11.017

A number of rhoptry proteins have been identified, including a complex of high molecular mass proteins containing three distinct polypeptides, RhopH1, RhopH2 and RhopH3 (the RhopH complex) [2–5]. The RhopH genes have been cloned from the human malaria parasite, *Plasmodium falciparum*, as well as the rodent malaria parasite, *Plasmodium yoelii* [6–10]. The *P. falciparum* RhopH (*Pf*RhopH) complex binds erythrocytes and distributes into the erythrocyte and parasitophorous vacuolar membranes [11,12]. *Pf*RhopH appears to be essential for parasite development: antibodies against the *Pf*RhopH complex partially inhibit growth of *P. falciparum* in vitro and in vivo [13–15], and attempts to disrupt the *Pf*RhopH3 gene locus were unsuccessful, suggesting a resulting lethal phenotype [16]. Taken together, these results strongly indicate that the RhopH complex has a critical role in erythrocyte invasion; however, the molecular interactions of this protein complex are poorly understood. For example, erythrocyte surface binding of the *P. falciparum Pf*RhopH complex was observed only with erythrocytes of the non-susceptible mouse, but not those of the susceptible human host, for which the RhopH complex receptor has not been identified.

To explore a biological role of the rhoptry proteins, we are focusing to characterize the erythrocyte receptors for the RhopH complex using a rodent malaria parasite. In this report we describe a flow cytometric-based erythrocyte binding assay and show that the *P. yoelii* RhopH complex specifically binds to erythrocytes of a susceptible mouse host. Using chimeric mice harboring GPI-deficient erythrocytes, we further show a possible role of the GPI-anchored protein for RhopH complex binding and determine that GPI-deficient erythrocytes are resistant to *P. yoelii* infection.

2. Materials and methods

2.1. Parasites and parasite extracts

Parasite infected blood was collected from *P. yoelii* 17X (lethal)-infected BALB/c mice and leukocytes were removed by passing through a CF11 column. Schizont-stage parasites were enriched by differential centrifugation over 50% Percoll (Amersham Pharmacia Biotech Inc., UK), washed twice in phosphate buffered saline (PBS), pH 7.4, and stored at −80 °C. Parasite proteins were extracted by three times repeated freeze-thaw at −80 °C from schizont-rich pellets in PBS, pH 7.4, containing protease inhibitors [PI; 1 μg ml^{-1} of leupeptin, 1 μg ml^{-1} of pepstatin A, 100 μM 4-(2-aminoethyl)benzenesulfonyl fluoride hydrochloride] and 1 mM EDTA (ethylenediaminetetraacetic acid), and a soluble fraction was obtained by centrifugation at 21,600 × *g* for 10 min to make a final concentration used for erythrocyte binding assays corresponding to 1×10^7 parasites μl^{-1}.

2.2. Monoclonal antibodies

The monoclonal antibodies mAb#25 (IgG1), #32 (IgG2b) and #16 (IgG1) recognizing *P. yoelii* RhopH2, RhopH3 and yPys25, respectively, were described [8,17].

2.3. Erythrocytes

Female BALB/c, DBA/2 and C57BL/6 (B6) mice were obtained from Charles River Japan Inc. GPA wild type (GPA$^{+/+}$) and knockout (GPA$^{-/-}$) mice and DARC wild type (DARC$^{+/+}$) and knockout (DARC$^{-/-}$) mice were generated and maintained in Tokyo University as described [18,19]. Mice harboring GPI-deficient erythrocytes were generated and maintained in Osaka University. Briefly, B6 mice were lethally irradiated and fetal liver cells were transplanted from mice with a disrupted *Pig-a* gene locus, which was essential for the GPI biosynthesis. Control mice were generated in a similar manner except that bone marrow was transplanted from a normal mouse [20]. Mouse blood was collected from tail snip bleeds into an excess amount of PBS containing 50 mM EDTA, washed extensively with PBS to remove serum and buffy coat, stored in PBS containing 1% bovine serum albumin (BSA), and used for binding assays within 1 day of preparation. Erythrocytes were also collected from two rabbits (JW/CSK; Japan SLC Inc., Japan) and two human donors (O-type/Rh-positive) by venous puncture and processed in a similar manner.

2.4. Erythrocyte enzyme treatments

Erythrocytes were incubated in RPMI1640 medium without sodium bicarbonate (designated as RPMI1640) with 1 mg ml^{-1} trypsin (Sigma, St. Louis, MO) or 1 mg ml^{-1} chymotrypsin (Sigma) for 2 h at 37 °C with gentle rocking. The erythrocytes were then washed once with RPMI1640, incubated with 1 mg ml^{-1} soybean trypsin inhibitor (STI; Sigma) or 10 mM *N*-p-Tosyl-L-phenylalanine chloromethyl ketone (TPCK; Sigma), respectively, for 10 min at room temperature (RT) with gentle rocking, and washed once with RPMI1640. Control erythrocytes were treated with STI or TPCK only.

Erythrocytes were also incubated with 100 or 200 mU ml^{-1} neuraminidase (1 U ml^{-1}; *Vibrio cholera*, CalBiochem, San Diego, CA) for 2 h at 37 °C and washed three times with RPMI1640. Two control treatments were devised as follows. In one tube, erythrocytes were incubated with a corresponding volume of the buffer. In a second tube, EDTA with a final concentration of 10 mM was added in addition to the neuraminidase solution, to inactivate neuraminidase activity by chelating calcium. Fluorescein isothiocyanate (FITC)-conjugated wheat germ agglutinin (WGA) recognizing *N*-acetylneuraminic acid (NANA) residues was used to monitor erythrocyte surface desialylation.

2.5. Erythrocyte binding assay

Approximately 1×10^7 erythrocytes were incubated in 100 μl of PBS with 10% BSA for 1 h, washed once with PBS, and further incubated in 100 μl of PBS containing 20 μl of *P. yoelii* extract for 30 min at RT, if specific volumes were not indicated. After centrifugation, the mixture was divided into erythrocyte pellets and supernatants containing unbound *P. yoelii* RhopH complexes. Supernatants were saved for later analysis to monitor RhopH complex protein degradation. Erythrocyte pellets were washed once with PBS and incubated with 1 μg of mAb#25, #32, or #16 for 15 min on ice, washed once with PBS, and incubated with 1 μg of FITC-conjugated goat anti-(mouse IgG and IgM) antibody (Biosource Int, Camarillo, CA) for 15 min on ice in 1 ml of PBS. After washing once with PBS, erythrocyte surface fluorescence was detected by flow cytometry. All experiments were done with duplicated samples and enzyme-treated erythrocytes were used in binding assays in the same day as treatment.

To distinguish GPI-deficient and GPI-positive erythrocyte populations, erythrocyte surface GPI anchor-associated CD24 was stained with rat anti-mouse CD24 mAb (BD Biosciences, San Jose, CA) and streptavidin-phycoerythrin (PE)-Cy5 (BD Biosciences). Erythrocytes from control normal mice were stained with or without anti-CD24 mAb and used as positive controls.

2.6. Flow cytometry analysis

Erythrocytes (1×10^7) were suspended in 1 ml of PBS and surface fluorescence intensities were measured by flow cytometry using a FACSCalibur™ (Becton Dickinson, NJ) flow cytometer and analyzed using the CellQuest™ software. First, single-parameter histograms were set for FITC fluorescence of cells within the scatter gate, with a gate set on the major erythrocyte population, and conditions were adjusted using untreated erythrocytes. Then, the geometric means of the fluorescence intensities were obtained for 10,000 erythrocytes incubated with or without *P. yoelii* extracts. Binding of the RhopH complex to the erythrocyte surface were given as a value obtained by dividing the geometric mean of fluorescence intensity of the experimental samples (with extract; INT_{exp}) by that of the control samples (without extract; INT_{ctl}).

For dual staining with FITC and PE-Cy5, erythrocytes were divided into two populations by PE-Cy5-fluorescence intensity and geometric mean of FITC fluorescence intensity increase were measured in these two populations independently.

2.7. SDS-PAGE, Western blot analysis, and immunoprecipitation

Parasite extracts were separated by electrophoresis on a 5–20% gradient polyacrylamide gel (ATTO, Japan) under non-reducing conditions and transferred to 0.22 μm PVDF membranes (Bio-Rad, Hercules, CA). Proteins were detected by immunostaining with corresponding antibodies, followed by horseradish peroxidase-conjugated goat antibody (anti-mouse IgG and IgM; Biosource Int) and visualized with ECL-plus (Amersham Biosciences) on RX-U film (Fuji, Japan).

To immunoprecipitate *Py*RhopH complexes, 50 μl of *P. yoelii* extract, 2 μl of yeast-produced recombinant Pys25 (yPys25) solution (5 mg ml^{-1}), and 2 μl (1 mg ml^{-1}) of mAb#32 were mixed and incubated at RT for 2 h with gentle rocking. Twenty microlitres of 50% Gamma Bind Plus Sepharose (Amersham Biosciences) solution were added and incubated another 1 h at RT with gentle rocking. The mixture was centrifuged at 21,600 × *g* for 5 min and supernatants were removed. The beads were washed in NETT [50 mM Tris (tris(hydroxymethyl)aminomethane)–HCl, 0.15 M NaCl, 1 mM EDTA, 0.5% Triton X-100, pH 7.5] + 1% BSA, NETT, high salt NETT (0.5 M NaCl), NETT, and 1/3 NETT (0.05 M NaCl and 0.17% Triton X-100). Supernatants were removed and bound proteins were eluted from beads by boiling at 100 °C for 3 min in 1× SDS-PAGE loading buffer and electrophoresed on a 5–20% gradient polyacrylamide gel under reducing and non-reducing conditions. As a control, mAb#16 was used to precipitate yPys25, instead of mAb#32.

2.8. Indirect immunofluorescence assay

A mouse harboring 28% GPI-deficient erythrocytes was inoculated intraperitoneally with *P. yoelii* 17X (lethal) and thin blood smears were prepared 3 days later at two time points. Blood smears were kept at −80 °C until use. Smears were fixed with 1% formaldehyde/PBS at RT for 15 min, blocked with 5% skim milk/PBS for 15 min at RT, reacted with rat anti-mouse CD24 mAb for 15 min at RT, washed with ice-cold PBS for 5 min, and reacted with FITC-conjugated goat anti-(rat IgG + IgM) mAb (BD Biosciences) for 15 min. Parasite nuclei were stained with DAPI (4′,6-diamidino-2-phenylindole; Wako) and mounted with Prolong Antifade solution (Molecular Probes, Eugene, OR). High-resolution image capture and processing were done using a fluorescence microscope (BX50; Olympus, Japan) and digital camera (IM500; Leica, Germany). Images were processed using Adobe Photoshop (Adobe Systems Inc., San Jose, CA).

2.9. Statistical analysis

The Mann–Whitney test was used to evaluate differences observed in erythrocyte binding assays. The chi-square test was used to evaluate the differences of parasite infectivity between GPI-positive and GPI-deficient erythrocytes. The Wilcoxon-Rank Sum test was used to evaluate the differences in parasite maturation.

3. Results

3.1. Flow cytometry analysis of PyRhopH complex interactions with erythrocytes

Prior to performing flow cytometry binding assays the character of parasite extracts was validated by Western blot analysis. *Py*RhopH2, *Py*RhopH3 and yPys25 [recombinant *Pys*25 protein (yPys25) was added to the parasite extracts as an internal control] could be detected by Western blot analysis using mAb#25, #32 and #16, respectively (Fig. 1A). *Py*RhopH1A and *Py*RhopH2 were co-precipitated using mAb#32, indicating that at least a partial RhopH complex is likely stable in the extract solution. *Py*RhopH1A, *Py*RhopH2 and *Py*RhopH3 were not co-precipitated with mAb#16 (Fig. 1B). Using parasite extracts the ability of *Py*RhopH complexes to bind normal, treated, and null erythrocytes was assessed by flow cytometry. Increased fluorescence intensity was detected using mAb#25 and #32 following incubation of BALB/c mouse strain erythrocytes with *P. yoelii* extract, in comparison to that without extract. No surface fluorescence increase was detected with mAb#16 recognizing control protein yPys25 (Fig. 1C). Fluorescence intensity increased in proportion to the amount of added *P. yoelii* extract, as shown in Fig. 1D.

3.2. PyRhopH complex binds specifically to mouse, but not rabbit or human erythrocytes

To determine the specificity of *Py*RhopH complex binding to erythrocytes, we examined binding using a panel of erythrocytes from other mouse strains [DBA/2 and B6], rabbit and human. The results were summarized in Table 1. Binding to DBA/2 and B6 mouse strain erythrocytes was similar to that from BALB/c mice. No binding was observed with rabbit or human erythrocytes with up to 50 μl of extract ($P < .01$). Thus *Py*RhopH complex recognized erythrocyte surface receptors from at least three different mouse strains, but not rabbit or human erythrocytes.

3.3. The erythrocyte PyRhopH complex receptor is sensitive to trypsin and chymotrypsin treatment

To characterize erythrocyte surface proteins involved in *Py*RhopH complex recognition, BALB/c and DBA/2 mouse erythrocytes were treated with trypsin or chymotrypsin. Both

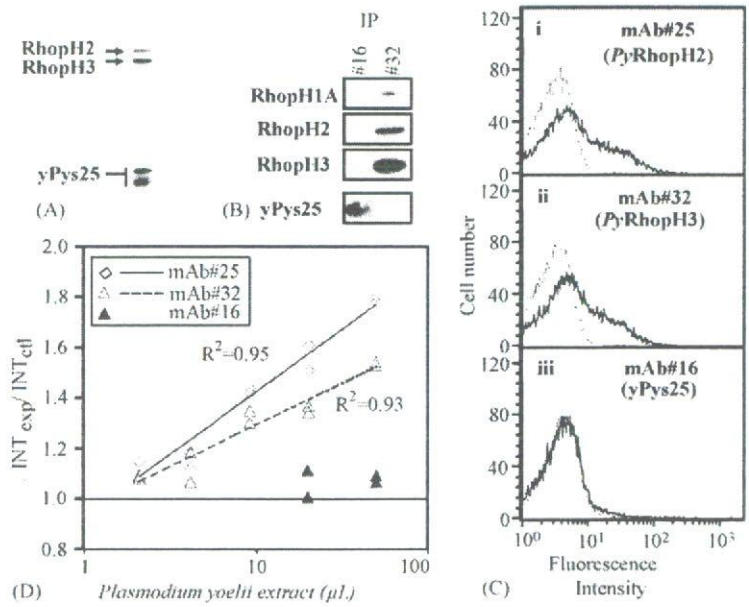

Fig. 1. *Py*RhopH complex binds mouse erythrocytes. (A) *P. yoelii* extracts were mixed with recombinant yPys25 (*Py*extract + yPys25) and subjected to Western blot analysis under non-reducing condition. The proteins were immunostained with mouse monoclonal antibodies mAb#25, #32 and #16, recognizing *Py*RhopH2, *Py*RhopH3 and yPys25, respectively. (B) Immunoprecipitation (IP) from *Py*extract + yPys25 with mAb#16 and #32 and immunostained with anti-*Py*RhopH1A mouse serum, mAb#25, #32 or #16, recognizing *Py*RhopH1A, *Py*RhopH2, *Py*RhopH3 or yPys25, respectively. The rhoptry protein complex was detected only with precipitants of mAb#32 but not mAb#16. (C) Mouse erythrocytes were incubated with *Py*extract + yPys25 (solid line) or PBS (broken line). RhopH complex binding was detected using mAb#25 or #32, followed by FITC-conjugated goat anti-(mouse IgG + IgM) antibody. A single-parameter histogram was set for FITC fluorescence of cells within the scatter gate, with a gate set on the major erythrocyte population. Fluorescence intensity increases (erythrocyte binding of *Py*RhopH complex) were observed for mouse erythrocytes with mAb#25 (i) and #32 (ii), but not with control mAb#16 that recognize yPys25 (iii). (D) The fluorescence intensity detected with mAb#25 and #32 for mouse erythrocytes increased in proportion to the amount of added *P. yoelii* extract. Representative data of multiple experiments are shown. Erythrocytes were incubated with 2, 4, 9, 20 and 50 μl of *P. yoelii* extracts and fluorescence intensity increases were measured. Geometric means were obtained for fluorescence intensities of 10,000 erythrocytes incubated with or without *P. yoelii* extract. RhopH complex binding to the erythrocyte surface was given as a value obtained by dividing the geometric mean of fluorescence intensity of the experimental sample (with extract; INT_{exp}) by that of the control sample (without extract; INT_{ctl}). Trendlines were drawn for these experiments, for which the coefficient of determination (R^2) were 0.95 (mAb#25) and 0.93 (mAb#32). Fluorescence intensities did not increase when mAb#16 was used.

Table 1
The *Py*RhopH complex binds erythrocytes of several mouse strains, but not human or rabbit erythrocytes

Erythrocyte		n[a]	INT_{exp}/INT_{ctl}[b]: median (range)	
Mouse	BALB/c	10	1.47 (1.10 – 1.80)	
	DBA/2	6	1.57 (1.38 – 1.84)	
	C57BL/6	8	1.39 (1.03 – 2.58)	
Rabbit	#1	10	0.995 (0.87 – 1.21)	c
	#2	4	0.99 (0.97 – 1.04)	
Human	#1	8	1.01 (0.95 – 1.07)	c
	#2	6	0.985 (0.94 – 1.04)	

[a] n indicates number of experiments and values were obtained from duplicated samples for each experiment. Data using mAb#25 were shown. Similar results were obtained using mAb#32 (not shown).
[b] *Py*RhopH complex binding to the erythrocyte surface were given as a value obtained by dividing the geometric mean of fluorescence intensity of the experimental samples (with extract; INT_{exp}) by that of the control samples (without extract; INT_{ctl}).
[c] Significant differences are indicated ($P < .01$).

Table 2
*Py*RhopH complex binding to mouse erythrocytes is abolished by trypsin- or chymotrypsin-treatment

Erythrocyte	INT_{exp}/INT_{ctl}[a]					
	mAb#25			mAb#32		
	BALB/c	BALB/c	DBA/2	BALB/c	BALB/c	DBA/2
Trypsin	0.97, 0.99	0.98, 1.04	0.99, 1.06†	0.91, 1.00	1.00, 1.00	0.97, 1.01†
Soy bean trypsin inhibitor	1.78, 1.91	1.24, 1.25	1.45, 1.47	1.75, 1.77	1.16, 1.19	1.25, 1.35
Chymotrypsin	0.97, 1.01	0.97, 0.97	1.00, 1.01†	1.04, 1.05	0.97, 0.98	0.98, 0.99†
TPCK	1.47, 1.52	1.09, 1.21	1.42, 1.57	1.40, 1.55	1.15, 1.27	1.33, 1.39

[a] *Py*RhopH complex binding to the erythrocyte surface were given as a value obtained by dividing the geometric mean of fluorescence intensity of the experimental samples (with extract; INT_{exp}) by that of the control samples (without extract; INT_{ctl}).
[b] Statistical differences ($P < .01$) are indicated between two groups using combined data from three experiments.

enzymes abolished *Py*RhopH complex binding ($P < .01$), indicating that a trypsin and chymotrypsin-sensitive erythrocyte receptor is likely involved in *Py*RhopH complex recognition (Table 2).

Involvement of the NANA component of erythrocyte surface proteins in *Py*RhopH complex recognition was evaluated using neuraminidase-treated erythrocytes. The efficiency of sialic acid removal was confirmed by the reduction of WGA lectin binding; specifically, to 17–24% or 20–24% of untreated erythrocytes following treatment of 100 or 200 mU ml^{-1} neuraminidase, respectively. Three independent experiments showed that *Py*RhopH binding was similar between controls and neuraminidase-treated erythrocytes, indicating that NANA was not involved in receptor recognition (not shown).

3.4. *PyRhopH complex binds to erythrocytes null for GPA and DARC*

Because the erythrocyte receptor is likely a membrane-associated protein, we were interested in determining if the known malaria parasite receptors GPA or DARC have roles as *Py*RhopH complex erythrocyte receptors. For these studies we used knockout mice disrupting these gene loci, in which the lack of the GPA or DARC expression have been confirmed [18,19]. Results of 4–5 independent experiments indicated that *Py*RhopH binding to GPA or DARC null erythrocytes was similar to binding of wild type erythrocytes, suggesting that neither GPA nor DARC are *Py*RhopH complex receptors (not shown).

3.5. *PyRhopH complex does not bind to the GPI-deficient mouse erythrocytes*

To evaluate the involvement of GPI anchors in *Py*RhopH complex binding, we used two mice harboring about 28% or 5% of GPI-deficient erythrocytes, which was determined with the surface expression of CD24. Erythrocytes from each mouse were separated into two groups based upon CD24-positivity, and *Py*RhopH complex bindings were independently measured. FL1 fluorescence intensity was increased for the GPI-positive population (Fig. 2A, upper), whereas it